SCIENCE CHINA
Information Sciences

• Supplementary File •

Nitrogen-vacancy-driven degradation mechanism in ferroelectric wurtzite AlScN

Ruiqing WANG[1], Jiuren ZHOU[1,2*], Xihui YUAN[1,2*], Feng ZHU[3], Siying ZHENG[1,2], Wenxin SUN[1], Xinghui WANG[1], Haiwen XU[1,2], Bochang LI[1,2], Yan LIU[1,2] & Genquan HAN[1,2]

[1]*Faculty of Integrated Circuit, Xidian University, Xi'an 710071, China*
[2]*Hangzhou Institute of Technology, Xidian University, Hangzhou 311200, China*
[3]*TRACE EM Unit and Department of Materials Science and Engineering, City University of Hong Kong, Hong Kong, China*

Appendix A Summary of sputtering parameters and thickness characterization of AlScN films

Table A1 Summary of the thickness for the AlScN thin films (Samples 1-4). The sputtering parameters and deposition time were maintained constant, whereas the gas composition was modulated by adjusting the Ar and N_2 flow rates.

	DC-Power (kW)	Base Pressure (Torr)	Temperature (°C)	Ar flow (sccm)	N_2 flow (sccm)	Time (s)	Thickness (nm)
Sample 1	10	4×10^{-7}	200	96	96	53	118
Sample 2	10	4×10^{-7}	200	64	128	53	106
Sample 3	10	4×10^{-7}	200	32	160	53	100
Sample 4	10	4×10^{-7}	200	0	192	53	94

* Corresponding author (email: zhoujiuren@xidian.edu.cn, yuanxihui@xidian.edu.cn)

Appendix B Semi-quantitative evaluation of nitrogen vacancies using EELS spectrum

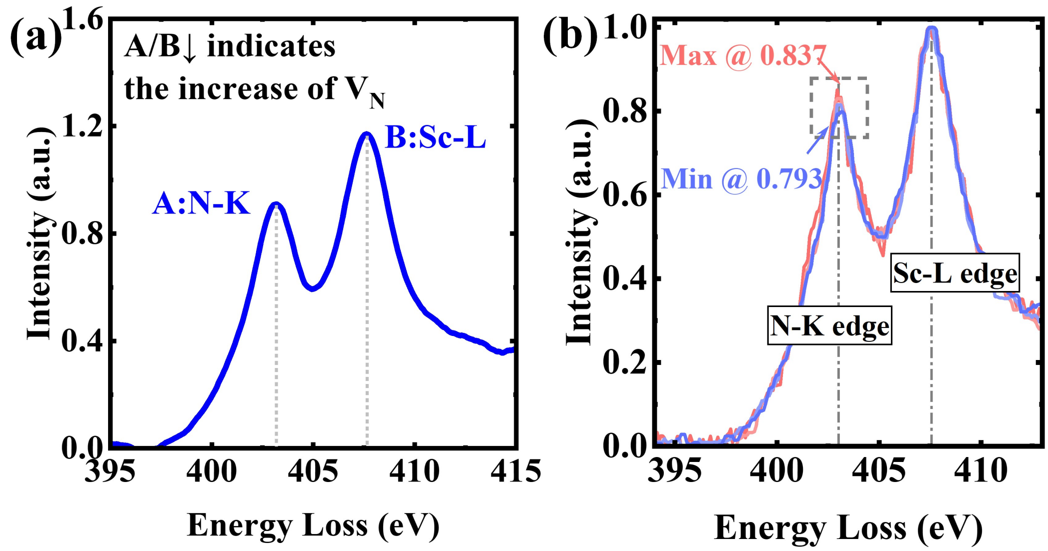

Figure B1 (a) EELS-derived N/Sc intensity ratio (N-K edge relative to Sc-L edge) for AlScN samples S1-S4 deposited under varied Ar:N_2 flow ratios, representing the relative V_N concentration. A lower N/Sc ratio corresponds to a higher V_N concentration. (b) Normalized EELS spectra of the N-K edge (centered at 403.1 eV), aligned to the Sc-L edge (407.5 eV) serving as an internal reference to ensure stoichiometric consistency. As the Ar:N_2 flow ratio is varied from 96:96 to 0:192 sccm, the N-K edge intensity increases from 0.793 to 0.837, indicating a progressive suppression of V_N.

Appendix C Quantitative analysis of nitrogen stoichiometry and oxygen impurity levels

Table C1 Energy Dispersive X-ray Spectroscopy (EDS) elemental composition of AlScN films (Samples 1-4). The results show a systematic increase in nitrogen percentage from 49.05% to 53.94% with higher N_2 flow. The oxygen content remains stable at a low level (∼2.5-3%), confirming that the material property changes are driven by nitrogen stoichiometry modulation rather than impurity fluctuations.

Ar:N_2 (sccm)	**N (%)**	**O (%)**
96:96	49.05	3.02
64:128	52.99	2.62
32:160	53.63	2.93
0:190	53.94	3.07

Appendix D Evolution of a-axis and c/a ratio in AlScN films with varied nitrogen ratio

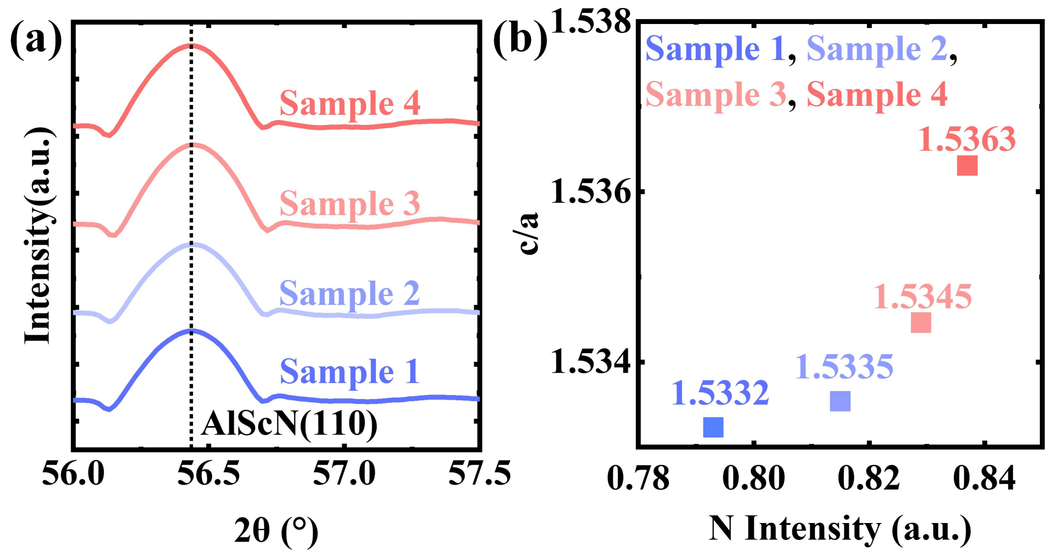

Figure D1 (a) XRD patterns of the (110) reflection for AlScN samples S1-S4 grown under different Ar:N_2 gas flow ratios. The negligible shift in peak position indicates that the in-plane (a-axis) lattice parameter remains nearly constant under all conditions. (b) Calculated c/a ratios, based on the corresponding (002) and (110) reflections, increase with higher nitrogen content, consistent with a suppressed V_N concentration and preferential lattice relaxation along the c-axis.

Appendix E Extraction of coercive field distribution via polarization derivative analysis

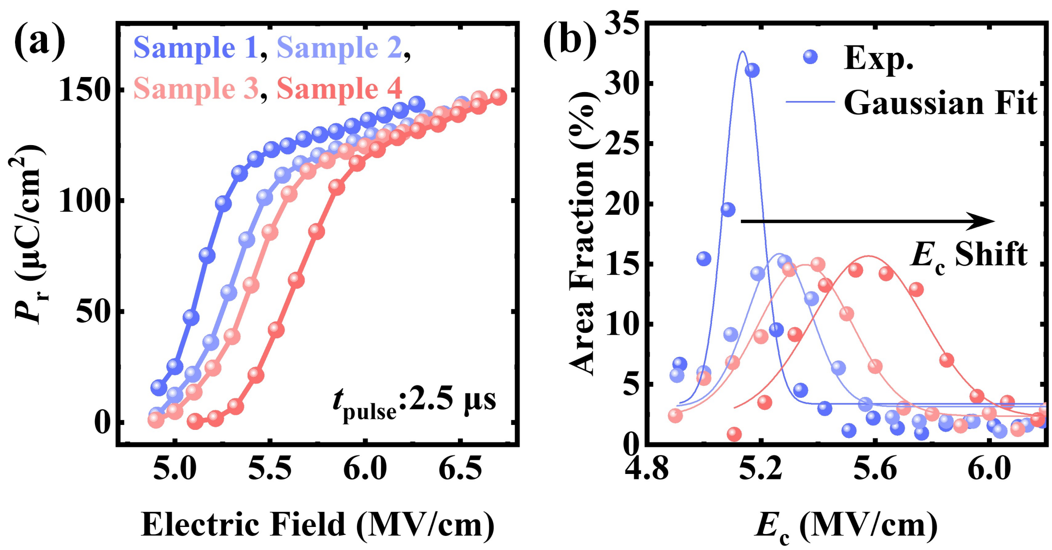

Figure E1 (a) A series of voltage pulses with progressively increasing maximum amplitude ($V_{\max}$) and a fixed width of 2.5 μs were applied to measure the P_r. (b) E_c distribution curves for AlScN films deposited under varied Ar:N_2 flow ratios. As the nitrogen content increases, the Gaussian peak progressively shifts toward higher values, indicating an increase in the average E_c. This shift is attributed to the suppression of defect-assisted nucleation. The reduction of V_N eliminates low-energy nucleation sites, thereby restoring the intrinsic high potential barrier for polarization switching.

Appendix F Suppression of nitrogen vacancies enhances coercive field and breakdown characteristics in AlScN films

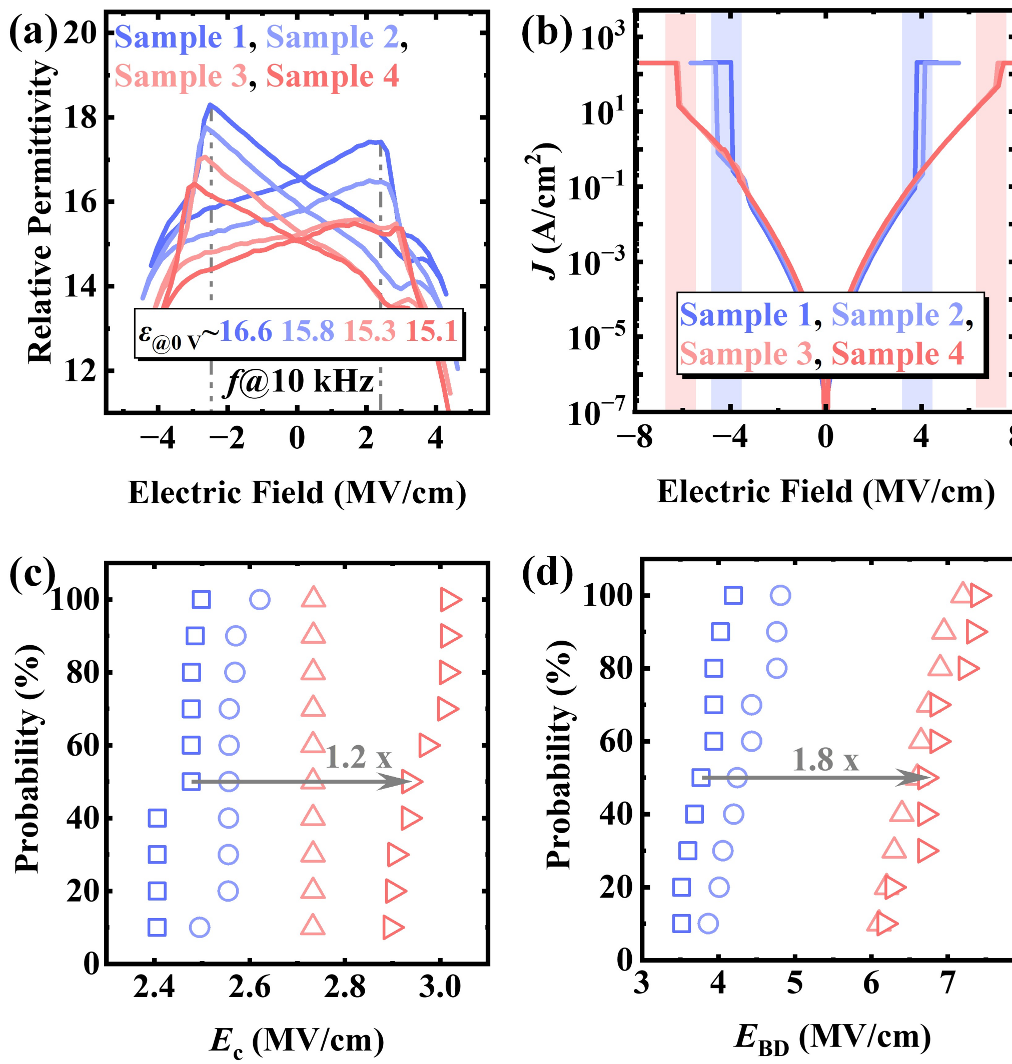

Figure F1 (a) C-V characteristics of four AlScN samples S1-S4 with different Ar:N_2 flow ratios. The E_c extracted from the inflection points of the C-V curves, increases systematically with nitrogen content. Simultaneously, the dielectric constant decreases, consistent with reduced V_N concentration. (b) Time-zero dielectric breakdown (TZDB) tests for samples S1-S4. A substantial increase in E_{BD} is observed with increasing nitrogen flow, confirming that suppression of V_N mitigates defect-assisted leakage and enhances dielectric robustness. (c) Statistical distribution of E_c values derived from C-V curves across ten devices per condition. The average E_c shows a 1.2× enhancement with increasing N_2 flow. (d) E_{BD} statistics for samples S1-S4 with varied V_N concentrations. A significant 1.8× enhancement in E_{BD} is observed with increasing N_2 flow, indicating that suppressing V_N effectively improves breakdown characteristics.

Appendix G Dual impact of nitrogen vacancies on energy barrier and breakdown strength

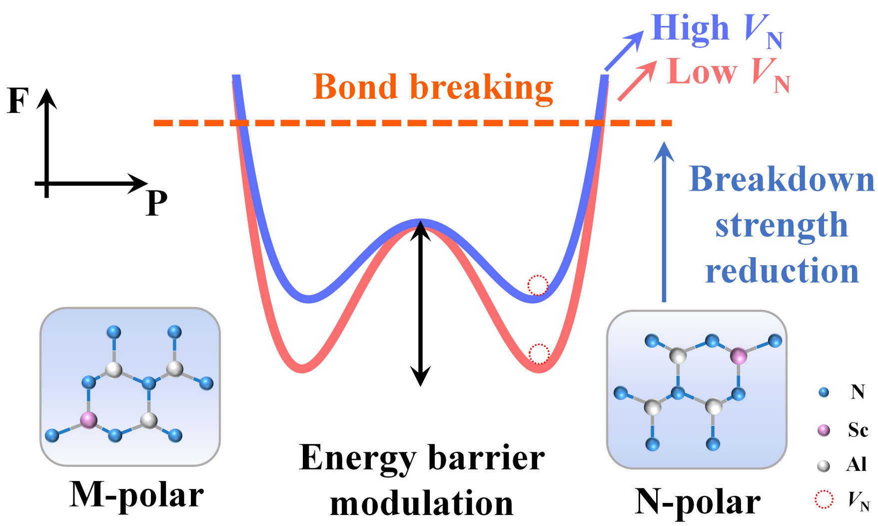

Figure G1 Schematic illustration of the Gibbs free energy (F) versus polarization (P) landscape. The comparison between high-$V_{\rm N}$ and low-$V_{\rm N}$ states demonstrates that nitrogen vacancies simultaneously lower the kinetic barrier for reducing $E_{\rm c}$ and the energy threshold for bond breaking, directly explaining the trade-off between facilitated switching and reduced breakdown strength.